THE JOURNAL OF IMMUNOLOGY

The NADPH Oxidase Pathway Is Dysregulated by the P2X $_7$ Receptor in the SOD1-G93A Microglia Model of Amyotrophic Lateral Sclerosis

Savina Apolloni, Chiara Parisi, Maria Grazia Pesaresi, Simona Rossi, Maria Teresa Carrì, Mauro Cozzolino, Cinzia Volonté and Nadia D'Ambrosi

J Immunol 2013; 190:5187-5195; Prepublished online 15 April 2013;
doi: 10.4049/jimmunol.1203262
http://www.jimmunol.org/content/190/10/5187

The Journal of Immunology is published twice each month by
The American Association of Immunologists, Inc.,
9650 Rockville Pike, Bethesda, MD 20814-3994.

Print ISSN: 0022-1767 Online ISSN: 1550-6606.

The NADPH Oxidase Pathway Is Dysregulated by the $P2X_7$ Receptor in the SOD1-G93A Microglia Model of Amyotrophic Lateral Sclerosis

Savina Apolloni,*,† Chiara Parisi,*,† Maria Grazia Pesaresi,† Simona Rossi,†,‡ Maria Teresa Carrì,†,‡ Mauro Cozzolino,†,§ Cinzia Volonté,*,† and Nadia D'Ambrosi*,†

Inflammation and oxidative stress are thought to play determinant roles in the pathogenesis of amyotrophic lateral sclerosis (ALS). Degenerating motor neurons produce signals that activate microglia to release reactive oxygen species (ROS) and proinflammatory cytokines, resulting in a vicious cycle of neurodegeneration. The ALS-causing mutant protein Cu^+/Zn^+ superoxide dismutase SOD1-G93A directly enhances the activity of the main ROS-producing enzyme in microglia, NADPH oxidase 2 (NOX2), a well-known player in the pathogenesis of ALS. Considering that extracellular ATP through $P2X_7$ receptor constitutes a neuron-to-microglia alarm signal implicated in ALS pathology, we used primary microglial cells derived from transgenic SOD1-G93A mice and SOD1-G93A mice lacking the $P2X_7$ receptor to investigate the effects of both pharmacological induction and genetic ablation of receptor activity on the NOX2 pathway. We observed that, in SOD1-G93A microglia, the stimulation of $P2X_7$ receptor by 2′-3′-*O*-(benzoyl-benzoyl) ATP enhanced NOX2 activity in terms of translocation of $p67^{phox}$ to the membrane and ROS production; this effect was totally dependent on Rac1. We also found that, following $P2X_7$ receptor stimulation, the phosphorylation of ERK1/2 was augmented in ALS microglia, and there was a mutual dependency between the NOX2 and ERK1/2 pathways. All of these microglia-mediated damaging mechanisms were prevented by knocking out $P2X_7$ receptor and by the use of specific antagonists. These findings suggest a noxious mechanism by which $P2X_7$ receptor leads to enhanced oxidative stress in ALS microglia and identify the $P2X_7$ receptor as a promising target for the development of therapeutic strategies to slow down the progression of ALS. ***The Journal of Immunology*****, 2013, 190: 5187–5195.**

Inflammation and oxidative stress are thought to play determinant roles in the pathogenesis of amyotrophic lateral sclerosis (ALS) (1). Degenerating motor neurons, the main pathological hallmark of ALS, produce signals that activate microglia, CNS-resident immune cells, to release free radicals and proinflammatory cytokines. This, in turn, causes further motor neuron stress and initiates a self-propagating cytotoxic cascade resulting in muscle weakness, atrophy, spasticity, and compromised speech, swallowing, and breathing (2, 3).

NADPH oxidase 2 (NOX2 or phagocytic oxidase-$gp91^{phox}$) is one of the major sources of extracellular and intracellular reactive oxygen species (ROS) in microglial cells, where it operates by transferring electrons across membranes from NADPH to molecular oxygen, generating $O_2^{\bullet -}$ (4). Activation of NOX2 in microglia increases both extracellular and intracellular ROS, causing neurotoxicity. The former are directly toxic to neurons, and the latter function as signals to amplify the production of several proinflammatory and neurotoxic cytokines through the activation of downstream molecules, including MAPK (i.e., p38 and ERK1/2) (5).

A central activator of NOX2 is the Rho-GTPase family member Rac1, acting as a molecular switch cycling between its inactive GDP-bound state and active GTP-bound state (6). GTP hydrolysis by Rac1 is controlled through a redox-dependent interaction with the ubiquitous enzyme Cu^+/Zn^+ superoxide dismutase (SOD1), which is found mutated in ALS patients. When SOD1 is bound to Rac1 under reducing conditions, GTP hydrolysis is inhibited; in oxidizing conditions, SOD1 dissociates from Rac1, no longer inhibiting GTP hydrolysis. The ALS-causing glycine-to-alanine substitution at position 93 (G93A) on SOD1 protein renders the enzyme less sensitive to redox uncoupling, leading to enhanced Rac1/NOX2 activation (7) and resulting in overproduction of damaging ROS (8). Consistently, NOX2 is upregulated in activated ALS microglia, and the deletion of NOX2 can improve disease progression and survival of SOD1-G93A mice (9–11). Furthermore, uncontrolled ROS, together with inflammatory cytokines produced by microglia, mediate disease progression, causing direct neurotoxicity and increasing motor neuron susceptibility to ALS-triggering factors (2, 12). Among these, extracellular ATP was recently suggested as a possible candidate. The role of extracellular nucleotides is well recognized in proliferation, chemotaxis, phagocytosis, and the release of proinflammatory molecules, namely in all aspects of microglia functioning (13). A major player in the response of microglia to extracellular ATP is the ionotropic purinergic $P2X_7$ receptor, which is responsible for the release of cytokines and induction of proinflammatory factors, such as TNF-α, IL-6, IL-1β, plasminogen, and cyclooxygenase-2 (COX-2) (14). Indeed, the proinflammatory function of $P2X_7$ receptor has

*Cellular Biology and Neurobiology Institute, National Research Council, Rome 00143, Italy; †Santa Lucia Foundation, Rome 00143, Italy; ‡Department of Biology, University of "Tor Vergata", Rome 00133, Italy; and §Institute of Translational Pharmacology, National Research Council, Rome, Italy

Received for publication November 27, 2012. Accepted for publication March 5, 2013.

This work was supported by Agenzia Italiana per la Ricerca sulla Sclerosi Laterale Amiotrofica (Grant PRALS 2009, cofinanced with the support of "5 × 1000," Healthcare Research of the Ministry of Health).

Address correspondence and reprint requests to Dr. Nadia D'Ambrosi, National Research Council/Santa Lucia Foundation, Via del Fosso di Fiorano 65, Rome 00143, Italy. E-mail address: n.dambrosi@hsantalucia.it

Abbreviations used in this article: ALS, amyotrophic lateral sclerosis; BBG, Brilliant Blue G; BzATP, 2′-3′-*O*-(benzoyl-benzoyl) ATP; COX-2, cyclooxygenase-2; MOI, multiplicity of infection; NOX2, NADPH oxidase 2; nt, nontransgenic; PAK, p21 activated kinase 1 protein; ROS, reactive oxygen species; SOD1, Cu^+/Zn^+ superoxide dismutase.

been involved in different neuropathologies with an inflammatory component, such as Alzheimer's and Huntington's diseases, multiple sclerosis, spinal cord injury, and neuropathic pain (15, 16). Recent articles reported that $P2X_7$ receptor expression and modulation are linked to neuroinflammation in human ALS and in different animal models for the disease (17, 18). In particular, human postmortem ALS spinal cord displays a greater density of $P2X_7$ receptor immunoreactivity in microglial cells, together with an increased production of COX-2 (19). A conspicuous $P2X_7$ receptor immunolabeling clearly delineating microglial cells was also present at advanced stages of disease in spinal cord sections of transgenic rats expressing mutant SOD1 (20). Thus, this distribution of $P2X_7$ receptor suggests its involvement in active microgliosis, which goes along with motor neuron degeneration in vivo. Consistently, in a previous study we showed that $P2X_7$ receptor mRNA and protein are upregulated in both primary and immortalized microglial cells from SOD1-G93A mice. As a functional consequence, the exposure of SOD1-G93A microglia to the $P2X_7$ receptor preferential agonist 2′-3′-*O*-(benzoyl-benzoyl) ATP (BzATP) amplified the morphological transition from resting/surveying to activated microglia and enhanced the content of TNF-α and COX-2. Furthermore, only microglia expressing SOD1-G93A protein and preactivated by BzATP displayed toxicity toward neuronal cells. All of these actions were prevented by the $P2X_7$ receptor–specific antagonist Brilliant Blue G (BBG), thus confirming the involvement of this receptor subtype in ALS (21). In a similar way, endogenous ATP and BzATP were later found to cause astrocyte-dependent neurotoxicity in culture, by inducing motor neuron death. Moreover, SOD1-G93A astrocytes displayed increased ATP-dependent proliferation and a basal increase in extracellular ATP degradation. Again, all of these events were prevented by BBG (22). Taken together, these results clearly suggest that the release/degradation of ATP and the activation of the $P2X_7$ receptor are involved in the microglia–astrocyte–motor neuron cross-talk that occurs during the progression of ALS.

The aim of this work is to define the molecular mechanisms within $P2X_7$ receptor activation that can account for an exacerbated response in SOD1-G93A microglia. In particular, we analyzed Rac1 and NOX2 activation and investigated upstream and downstream signaling mechanisms. To ascertain unequivocally the role of $P2X_7$ receptor in the microglial inflammatory pathway, we took advantage of both pharmacological and molecular inhibition of $P2X_7$ receptor activity by using different antagonists and generating SOD1-G93A mice lacking this receptor.

Materials and Methods

Generation of $P2X_7^{-/-}$/SOD1-G93A transgenic mice

Adult B6.Cg-Tg(SOD1-G93A)1Gur/J mice expressing a high copy number of mutant human SOD1 with a $Gly^{93}Ala$ substitution (SOD1-G93A) and B6.129P2-P2rx7^{tm1Gab}/J mice ($P2X_7^{-/-}$) were originally obtained from The Jackson Laboratory (Bar Harbor, ME) and bred in the indoor animal facility, where they were kept until experiments were carried out. SOD1-G93A transgenic animals were crossed with background-matched B6J wild-type females, and selective breeding maintained each transgene in the hemizygous state. Nontransgenic (nt) littermate mice were used as controls. To generate SOD1-G93A mice lacking the $P2X_7$ receptor ($P2X_7^{-/-}$/SOD1-G93A), SOD1-G93A males were first cross-bred with $P2X_7^{-/-}$ females to generate F1 progeny ($P2X_7^{+/-}$/SOD1-G93A), and the $P2X_7^{+/-}$/SOD1-G93A males were cross-bred with $P2X_7^{-/-}$ females to obtain the F2 progeny ($P2X_7^{-/-}$/SOD1-G93A). All transgenic mice were identified by analyzing tissue extracts from tail tips. Animals were housed at constant temperature (22 ± 1°C) and relative humidity (50%) with a regular 12-h light cycle (light 7 AM–7 PM) throughout the experiments. Food and water were freely available. All animal procedures were performed according to the European Guidelines for the use of animals in research (86/609/CEE) and the requirements of Italian laws (D.L. 116/92). The ethical procedure was approved by the Animal Welfare Office, Department of Public Health and Veterinary, Nutrition and Food Safety, General Management of Animal Care and Veterinary Drugs of the Italian Ministry of Health. All efforts were made to minimize animal suffering and to use only the number of animals necessary to produce reliable results.

Reagents

BzATP, BBG, and all other reagents, unless otherwise stated, were obtained from Sigma-Aldrich (Milan, Italy). PD98059 and catalase (bovine liver) were purchased from Calbiochem (San Diego, CA). A-839977 and A-438079 were from Tocris Bioscience (Bristol, U.K.).

Abs

$P2X_7$ rabbit polyclonal Ab (1:500) was purchased from Alomone Labs (Jerusalem, Israel); Rac1 mouse Ab (1:1000) was obtained from Millipore (Merck Millipore, Merck KGaA, Darmstadt, Germany); $p67^{phox}$ (1:200 for immunofluorescence and 1:500 for Western blot) and $gp91^{phox}$ (1:1000–1:2000) mouse mAbs were from BD Transduction Laboratories (Lexington, KY); p44/42 MAPK (ERK1/2; L34F12; 1:2000) mouse Ab and phospho-p44/42 MAPK (ERK1/2; Thr202/Tyr204; 1:1000) and phospho-p38 MAPK (Thr180/Tyr182; 12F8; 1:700) rabbit Abs were from Cell Signaling Technology (Beverly, MA). HRP-linked anti-rabbit and anti-mouse Abs were from Cell Signaling Technology.

Primary microglia cell cultures

Mixed glial cultures from brain cortex were prepared as we described previously (21). Briefly, neonatal SOD1-G93A, $P2X_7^{-/-}$/SOD1-G93A, and nt mice were sacrificed; after removing the meninges, cortices were minced and digested with 0.01% trypsin and 10 μg/ml DNase I. After dissociation and passage through 70-μm filters, cells were resuspended in DMEM/F-12 media with GlutaMAX (Life Technologies, Invitrogen, Paisley, U.K.) plus 10% FBS, 100 U/ml gentamicin, and 100 μg/ml streptomycin/penicillin at a density of 62,500 cells/cm^2. After ∼15 d, a mild trypsinization (0.08% trypsin in DMEM/F-12 without FBS) was performed for 40 min at 37°C to remove nonmicroglial cells (23). The resultant adherent microglial cells (>99% pure) were washed twice with DMEM/F-12 and kept in 50% mixed glial cell–conditioned medium at 37°C in a 5% CO_2 and 95% air atmosphere for 48 h until use.

Protein extraction, SDS-PAGE, and Western blotting

To isolate total-protein extracts, cells in serum-free medium were harvested in ice-cold RIPA buffer (PBS, 1% Nonidet P-40, 0.5% sodium deoxycholate, 0.1% SDS) added to protease inhibitor mixture (Sigma-Aldrich). Lysates were kept on ice for 30 min and then centrifuged for 10 min at 14,000 × *g* at 4°C. Supernatants were collected and assayed for protein quantification with the BCA protein assay (Thermo Fischer Scientific, Rockford, IL). Analysis of protein components was performed using Mini-PROTEAN TGX Gels (Bio-Rad Laboratories, Milan, Italy) and transfer onto nitrocellulose membranes (Amersham Biosciences, Cologno Monzese, Italy). After saturation with ECL Advance Blocking Agent (Amersham Biosciences), blots were probed overnight at 4°C with the specified Ab, incubated for 1 h with HRP-conjugated secondary Abs, and detected on x-ray film (Aurogene, Rome, Italy), using an ECL Advance Western Blotting Detection Kit (Amersham Biosciences). Quantifications were performed using a Kodak Image Station.

Membrane translocation of $p67^{phox}$

After drug treatment, primary microglia were lysed in relaxation buffer (100 mM KCl, 3 mM NaCl, 3.5 mM $MgCl_2$, 1.25 mM EGTA, and 10 mM PIPES [pH 7.3]) added to protease inhibitor mixture (Sigma-Aldrich) and sonicated (3 × 10 s, at 4°C using an ultrasonic processor [Hielscher, Teltow, Germany]). Cell lysate was centrifuged at 500 × *g* to remove mitochondria and nuclei, generating a postnuclear supernatant that was subsequently ultracentrifuged at 100,000 × *g* for 1 h at 4°C to spin down total membranes. The membrane fraction was resuspended in 100 μl relaxation buffer added to 1% Triton X-100, protein concentration was estimated using BCA assay, and 5 μg protein was analyzed using Western blot with anti-$p67^{phox}$ Ab. To normalize the total amount of cell membranes, Western blot with an Ab recognizing the mouse NOX2 membrane–resident $gp91^{phox}$ subunit was performed.

Rac1 constructs, transfection, and virus transduction

Human cDNA coding for Rac1 (GenBank accession number NM_006908) was cloned by RT-PCR from human SH-SY5Y neuroblastoma cells using

the forward primer 5′-AAA GGA TCC ATG CAG GCC ATC AAG TGT G-3′ and the reverse primer 5′-AAA TCT AGA TTA CAA CAG CAG GCA TTT TCT C-3′. The resulting PCR fragment was inserted into BamHI/XbaI restriction sites of pRRLSIN.cPPT.PGK-eGFP lentiviral vector. Rac1-V12 and Rac1-N17 were produced by PCR site-directed mutagenesis using wild-type Rac1 plasmid as a template, followed by digestion with Dpn1. All of the pRRLSIN.cPPT.PGK-eGFP constructs were verified by automated sequencing and then purified and cotransfected together with packaging vectors into HEK-293FT cells. Supernatants were collected after 48 and 72 h, and viral particles were concentrated by ultracentrifugation for 2 h at 26,000 rpm (Ultraclear Tubes, SW28 rotor, and Optima l-100 XP Ultracentrifuge; Beckman Coulter, Milan, Italy) and recovered by suspension in HBSS (Sigma-Aldrich). Titers of viral particles ranged between 10^6 and 10^7 TU/ml. Viral particles and polybrene (8 μg/ml final concentration) were then added to isolated primary microglia. Lentiviral particles, at a multiplicity of infection (MOI) of 30, and 8 μg/ml polybrene (Sigma-Aldrich) were added to the culture. Supernatant was removed 5 h postinfection and replaced with DMEM-F12 medium containing 10% FBS. In all of the experiments, the efficiency of microglia transduction was ≥90%, as determined by counting the number of microglia expressing the GFP molecule and counterstaining nuclei with Höechst 33258 (1 μg/ml for 5 min) by means of a fluorescent microscope. Cell morphology was visualized by Cy3-conjugated phalloidin staining (5 μg/ml). GFP–adenovirus construction was described previously (24) and used at an MOI of 30–50. All experiments were performed at 72 h postinfection.

Rac1 pull-down assay

The Rac-GTP pull-down assay was performed as previously described (24). Briefly, cells were lysed in a buffer containing 50 mM Tris [pH 7.2], 100 mM NaCl, 5 mM $MgCl_2$, 1 mM DTT, 10% glycerol, and 1% Nonidet-P40 plus protease inhibitors. One fiftieth of the cell lysate was subjected to Western blotting. Cell lysates were mixed with 10 mg bacterially expressed GST-p21 activated kinase 1 protein (PAK) (rat PAK aa 1–252) bound to glutathione-Sepharose and incubated at 4°C with tumbling for 30 min. Beads were collected by centrifugation and washed twice in lysis buffer prior to the addition of Laemmli buffer and analysis with anti-Rac1 Ab by Western blot.

Intracellular ROS measurement

Because of the many limitations of standard fluorescent probes when measuring intracellular ROS by fluorescence microscope analysis (25), intracellular production of ROS was measured by monitoring the oxidation of the cell-permeable nonfluorescent reagent CellROX Deep Red Reagent (Molecular Probes, Carlsbad, CA), which, upon oxidation, exhibits a strong fluorogenic signal that is stable after fixation. Briefly, 2×10^5 cells were starved with serum-free medium and then exposed to treatments. Subsequently, cells were incubated with 5 μM CellROX Deep Red Reagent and 1 μg/ml Höechst 33258 (for nuclei) for 30 min at 37°C and, after three washes with PBS, were fixed for 10 min in 4% paraformaldehyde. Cells were mounted and cover-slipped with Gel/Mount antifading (BioMeda, Burlingame, CA). Fluorescence was analyzed using a confocal laser scanning microscope (LSM700; Zeiss, Oberkochen, Germany) equipped with four laser lines: 405, 488, 561, and 639 nm. Images were analyzed with ImageJ software.

H_2O_2-production assay

Microglial cells were grown in 96-well fluorescence tissue culture plates at a density of 10^4 cells/well. After treatment, an Amplex Red Hydrogen Peroxide/Peroxidase Assay (Molecular Probes) was performed to detect H_2O_2 released from cells. In the presence of HRP, the Amplex Red reagent (10-acetyl-3,7-dihydroxyphenoxazine) reacts with H_2O_2 in a 1:1 stoichiometry to produce the red-fluorescent oxidation product resorufin. Fluorescence was recorded from the blank, control, and treated cells, together with a positive control, in a multilabel counter (Victor3-V; PerkinElmer Life Sciences, Milan, Italy) by measuring ($530–560_{Ex}/590_{Em}$) fluorescence every 5 min over the experimental time period. To normalize the cell number, the CellTiter-Blue Cell Viability Assay (Promega Italia, Milan, Italy) was then performed. Briefly, after incubating cells with the CellTiter-Blue Reagent, fluorescence was recorded in the same multilabel counter at the same experimental excitation and detection ($530–560_{Ex}/590_{Em}$).

Immunofluorescence microscopy

SOD1-G93A and $P2X_7^{-/-}$/SOD1-G93A primary cells were fixed for 15 min in 4% paraformaldehyde and permeabilized for 5 min in PBS containing 0.1% Triton X-100. The cells were then incubated for 1.5 h at 37°C with mouse anti-$p67^{phox}$ (1:200; BD Biosciences) in 1% BSA in PBS. The cultures were stained for 1 h with Cy2-conjugated donkey anti-mouse IgG (1:200; Jackson ImmunoResearch, West Grove, PA). Nuclei were stained with 1 μg/ml Höechst 33258 for 5 min, and the cells were mounted and cover-slipped with Gel/Mount antifading (BioMeda). Immunofluorescence was analyzed using a confocal microscope, as described above.

Data analysis

Data are presented as mean ± SEM. Statistical differences were verified by the Student *t* test using MedCalc (Medcalc Software, Mariakerke, Belgium), followed by individual post hoc comparisons (Fisher protected least significant difference). The p values < 0.05 were considered significant.

Results

Modulation of $P2X_7$ receptor affects $p67^{phox}$ subunit translocation

To investigate the modulation of the NOX2 pathway by $P2X_7$ receptor activation in SOD1-G93A microglia, we first examined the translocation of the NOX2 activator $p67^{phox}$ to cell membranes. As shown in Fig. 1A, under basal conditions, SOD1-G93A microglia display a higher amount of membrane-associated $p67^{phox}$ with respect to cells derived from nt animals (normalized to the membrane-resident $gp91^{phox}$ subunit). Activation of the $P2X_7$ receptor by addition of BzATP increases the presence of $p67^{phox}$ in membranes of both nt and SOD1-G93A cells. However, 10 μM BzATP increases $p67^{phox}$ subunit translocation ~3.5-fold (with respect to nt cells) only in SOD1-G93A microglia, whereas a higher BzATP concentration (100 μM) results in only a 2-fold increase in the $p67^{phox}$ subunit in membranes of nt cells and a 4-fold increase in SOD1-G93A cells. The translocation of $p67^{phox}$ in SOD1-G93A membranes by BzATP was confirmed by immunofluorescence (Fig. 1B), because the generally diffused cytosolic staining of anti-$p67^{phox}$ Ab becomes enriched on cell membranes upon 100 μM agonist stimulation. This effect is completely prevented by the addition of BBG, A-839977, or A-438079 (all at 1 μM), as shown by immunofluorescence and Western blotting (Fig. 1B, 1C). Thus, the effectiveness of BzATP and the inhibition by specific antagonists indicate that the $P2X_7$ receptor mediates the translocation of $p67^{phox}$. Indeed, in SOD1-G93A microglia in which the $P2X_7$ receptor is knocked out (Fig. 1D, *left panel*), stimulation with 100 μM BzATP fails to increase $p67^{phox}$ in cell membranes, as demonstrated by immunofluorescence and Western blotting (Fig. 1D). These data reinforce the $P2X_7$ receptor as a likely candidate to modulate the NOX2 pathway in ALS microglia (Fig. 8).

$P2X_7$ receptor influences GTP-bound Rac1 level

The Rho-GTPase family member Rac1 is a central activator of NOX2 via a multistep mechanism involving binding to GTP, translocation to cell membrane and direct interaction with $gp91^{phox}$, followed by a subsequent interaction with $p67^{phox}$ (26). Thus, we analyzed the effect of BzATP on Rac1 activation in nt and SOD1-G93A microglia by measuring GTP-bound active Rac1 with a GST-PAK1 pull-down assay (Fig. 2). Western blot analysis of pulled-down Rac1 shows that, already under unstimulated conditions, SOD1-G93A microglia display a 3-fold higher amount of GTP-Rac1 than do nt cells, as normalized to the expression of total Rac1. Despite this elevated Rac1 activity under basal conditions, the addition of BzATP at 10 μM and at 100 μM is able to dramatically increase the content of active Rac1 in SOD1-G93A microglia compared with unstimulated nt cells (3- and 6-fold, respectively) and with stimulated nt cells (3-fold in each case). With regard to $p67^{phox}$ translocation, the addition of 1 μM BBG (Fig. 2A, *left panel*, 2B) or the molecular deletion of $P2X_7$ receptor (Fig. 2A, *right panel*) completely abolishes Rac-1 activa-

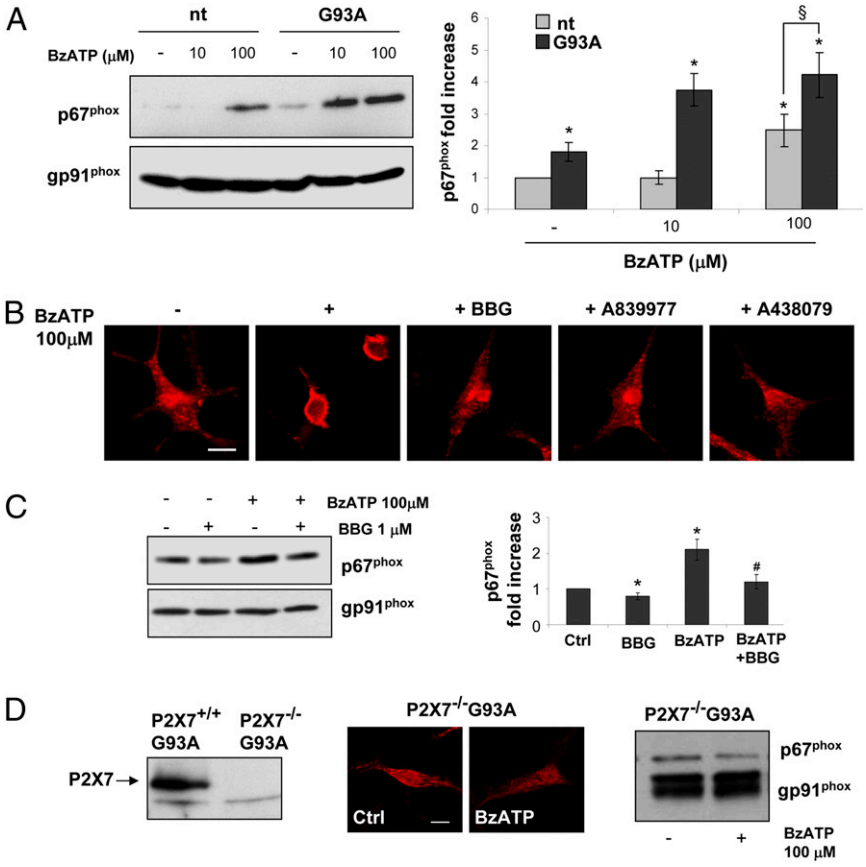

FIGURE 1. P2X$_7$ receptor modulates the translocation of p67^{phox}. (**A**) SOD1-G93A and nt microglia were exposed to 10 or 100 μM BzATP for 10 min, and equal amounts of isolated plasma membranes were subjected to SDS-PAGE, Western blotting, and immunoreactions with anti-p67^{phox} and anti-gp91^{phox} (1:2000) to normalize membrane proteins. SOD1-G93A cells pretreated with 1 μM BBG, A-839977, or A-438079 and then exposed to 100 μM BzATP for 10 min were analyzed by confocal microscopy after fixation, permeabilization, and staining with anti-p67^{phox}, followed by Cy3-conjugated donkey anti-mouse IgG (**B**), or by Western blot, performed as above (**C**). Data represent mean ± SEM of $n = 3$ independent experiments. (**D**) Western blotting of SOD1-G93A and P2X$_7^{-/-}$/SOD1-G93A microglia with anti-P2X$_7$ receptor Ab (*left panel*). P2X$_7^{-/-}$/SOD1-G93A microglia were treated with 100 μM BzATP for 10 min, and p67^{phox} membrane translocation was analyzed by confocal microscopy (*middle panels*) and by Western blotting with anti-p67^{phox} and anti-gp91^{phox} (1:1000) to normalize membrane proteins (*right panel*). Scale bars, 50 μm. $^{*}p < 0.05$ versus nt untreated cells, $^{§}p < 0.05$ versus 100 μM BzATP–treated nt cells, $^{\#}p < 0.05$ versus 100 μM BzATP–treated SOD1-G93A cells, Student *t* test.

tion by 100 μM BzATP in SOD1-G93A microglia. Most importantly, active Rac1 is significantly decreased by BBG in SOD1-G93A microglia, even in the absence of P2X$_7$ receptor exogenous stimulation (Fig. 2A, *left panel*, 2B), suggesting, overall, that basal P2X$_7$ receptor activity contributes to the Rac1-NOX2 detrimental pathway in ALS microglia.

NOX2 activation by P2X$_7$ receptor is Rac1 dependent

To determine the dependency of the P2X$_7$ receptor/NOX2 pathway on Rac1 recruitment in SOD1-G93A microglia, we made use of SOD1-G93A microglia transduced with two Rac1 mutants. Microglia are very sensitive to activation as a consequence of experimental manipulations. To preserve their resting state, despite high-efficiency transduction of Rac1 mutants, we first compared lentiviral and adenoviral infections of microglia. As shown by green fluorescence (Fig. 3A), infection with lenti-GFP results in ~80% efficiency, whereas the adeno-GFP yield is ~60%. Moreover, as indicated by Western blot analysis, infection with lenti-GFP does not modify the expression of CD68, a marker for active microglia, whereas adeno-GFP results in a 2-fold increase in CD68 expression (Fig. 3A). Thus, we used lentiviral infection to transduce a constitutively active (V12) and a dominant inactive (N17) form of Rac1 and measured the translocation of p67^{phox} in membrane. As expected, the infections with mutated Rac1 constructs give rise to modifications of cellular morphology (Fig. 3B), because Rac1 is a regulator of actin cytoskeleton organization (27). In the presence of V12 Rac1, microglia show smaller cell bodies becoming characteristically amoeboid, whereas the expression of N17 Rac1 mutant reduces the cell bodies and transforms the long cellular protrusions of control cells into a more spiny phenotype (Fig. 3B). The membrane levels of p67^{phox} are increased in the presence of V12 Rac1, where cells show an active phenotype, whereas in the presence of N17 Rac1, the amount of membrane-bound p67^{phox} is comparable to GFP-infected cells. Differently from GFP-infected control cells, the addition of 100 μM BzATP does not increase NOX2 activity when cells are transduced with any exogenous constitutively active or dominant-

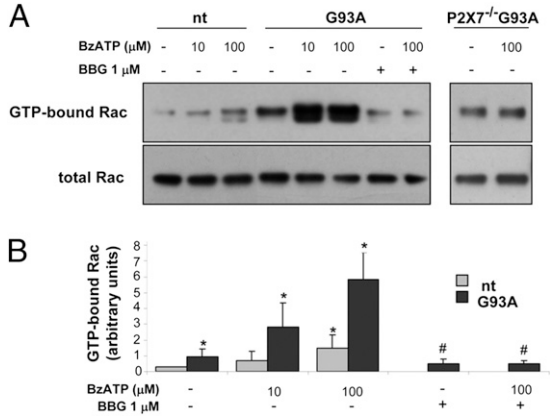

FIGURE 2. GTP-bound Rac1 levels are regulated by the P2X$_7$ receptor. SOD1-G93A, P2X$_7^{-/-}$/SOD1-G93A, and nt microglia were pretreated or not with 1 μM BBG and then treated with BzATP (10–100 μM) for 1 min. (**A**) GTP-bound Rac1 was pulled down by a GST-PAK protein, conjugated to GSH-Sepharose. The GTP-bound and the total amount of GTPases, used for normalization, were detected by Western blotting using the anti-Rac1 Ab. (**B**) Data were quantified and represent mean ± SEM of $n = 3$ independent experiments. $^{*}p < 0.05$ versus nt untreated cells, $^{\#}p < 0.05$ versus 100 μM BzATP–treated SOD1-G93A cells, Student *t* test.

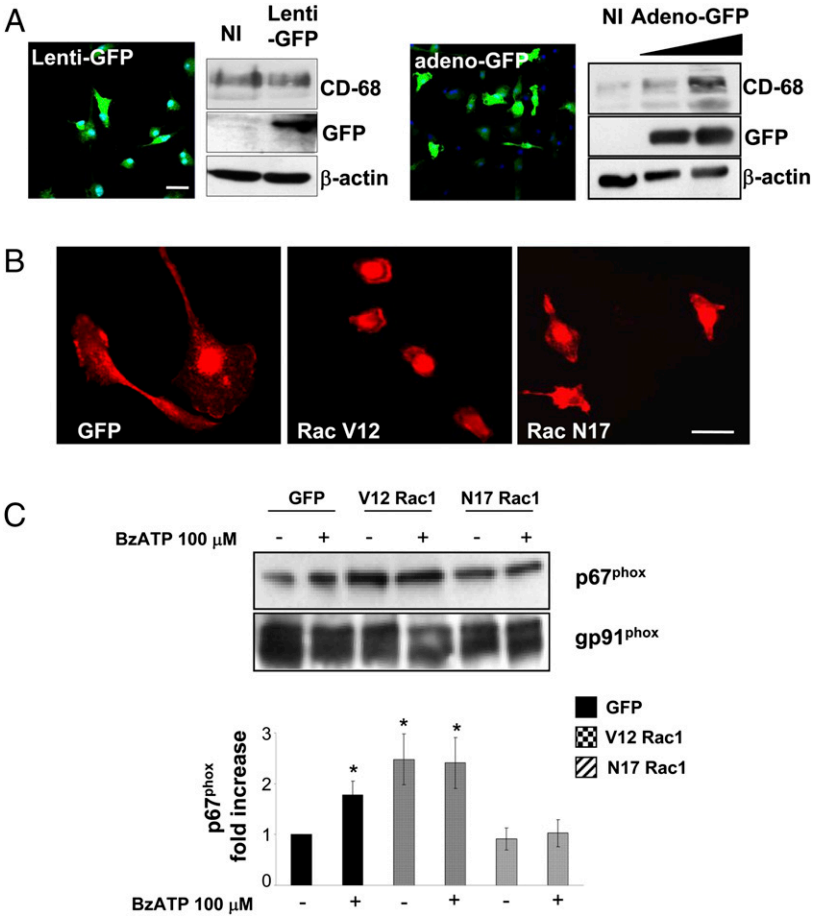

FIGURE 3. NOX2 stimulation by the $P2X_7$ receptor relies on Rac1 activity. (**A**) SOD1-G93A microglia were infected with lentiviral (Lenti)-GFP particles at an MOI of 30 (*left panels*), or with adenoviral (Adeno)-GFP particles at an MOI of 30 and 50 (*right panels*). In both conditions, GFP^+ cells were visualized, and nuclei were counterstained with Höechst 33258 (blue), using a fluorescent microscope. Equal amounts of total lysates from infected microglia were subjected to SDS-PAGE, Western blotting, and immunoreactions with anti-CD68 and anti–β-actin for protein normalization. SOD1-G93A microglia infected with lentiviral particles carrying Rac1 mutants were either fixed and stained with phalloidin (red) (**B**), or they were stimulated with 100 μM BzATP and subjected to membrane isolation, followed by SDS-PAGE, Western blotting, and immunoreactions with anti-$p67^{phox}$ and anti-$gp91^{phox}$ (1:1000) Abs to normalize membrane proteins (**C**). Data represent mean ± SEM of $n = 3$ independent experiments. Scale bars, 50 μm. $^*p < 0.05$ versus cells infected with lentiviral particles carrying only GFP, Student t test. NI, Noninfected cells.

negative form of Rac1 (Fig. 3B), demonstrating that NOX2 activation by the $P2X_7$ receptor, in terms of $p67^{phox}$ membrane translocation, is totally dependent on Rac1 recruitment and not on alternative pathways (Fig. 8).

Modulation of $P2X_7$ receptor affects ROS production

Because the activity of NOX2 results in the generation of ROS, we investigated the effect of $P2X_7$ receptor modulation on the production of ROS in nt and SOD1-G93A microglia. As shown in the time-course experiments in Fig. 4A, ROS production (measured as H_2O_2 content) stimulated by BzATP peaks at 10 min and then reaches a plateau. Consistent with activation of the NOX2 complex, 10 μM BzATP fails to stimulate ROS production in nt cells, but it results in a clear increase in ROS in SOD1-G93A microglia; when used at 100 μM, BzATP enhances the production of ROS to a significantly higher extent in SOD1-G93A microglia than in nt cells (2- and 1.3-fold, respectively, over untreated cells) (Fig. 4A, 4B). To ascertain whether ROS were generated by NOX2 activity, we stimulated microglial cells in the presence of apocynin, an inhibitor of the translocation of NOX2 cytoplasmic subunits (Fig. 4B). The addition of 250 μM apocynin prior to 100 μM BzATP results in 70% inhibition of ROS produced by SOD1-G93A microglia, suggesting NOX2 as a major source of ROS induced by BzATP. We also investigated ROS production by fluorescence analysis of the oxidative dye CellROX Deep Red Reagent in SOD1-G93A microglia stimulated with 100 μM BzATP, in the absence or presence of 50 U/ml catalase (to neutralize H_2O_2 possibly released in the medium), or of the antagonists BBG, A-839977, or A-438079 (all at 1 μM). As shown in Fig. 4C, although almost all of the cells (~90%) are stained after treatment with BzATP, even in the presence of catalase, preincubation with the antagonists reduces CellROX Deep Red Reagent intensity down to control levels. These data indicate that BzATP stimulates ROS production via the $P2X_7$ receptor and primarily via NOX2 activity (Fig. 8).

ERK1/2, but not p38 MAPKs, are differently recruited by $P2X_7$ receptor stimulation in SOD1-G93A microglia compared with nt microglia

It is well established that intracellular ROS function as signaling molecules in microglia to amplify the production of several proinflammatory and neurotoxic cytokines. This is achieved through several downstream-signaling molecules, such as MAPK (i.e., p38 and ERK1/2) (5). Moreover, it was reported that, upon proper stimuli, these same kinases can be recruited upstream of NOX2 in the phosphorylation of $p47^{phox}$ and $p67^{phox}$, an event necessary for the translocation of these subunits to membranes. To dissect the signaling pathway leading to the increased response of SOD1-G93A microglial cells to BzATP, we investigated the phosphorylation of p38 and ERK1/2. Fig. 5A shows that 100 μM BzATP activates p38 with comparable kinetics in both nt and SOD1-G93A microglia: the expression of p-p38, normalized to total ERK1/2, peaks at 2.5 min and starts decreasing thereafter. Again, this effect is mediated specifically by the $P2X_7$ receptor, because the addition of 1 μM BBG or ablation of the $P2X_7$ receptor inhibits the upregulation of p-p38 in SOD1-G93A microglia (Fig. 5B) and nt cells (data not shown). Thus, $P2X_7$ receptor stimulation induces a similar time- and dose-dependent p38 activation in nt and SOD1-G93A microglia. With the aim to ascertain whether this event is upstream of NOX2, as suggested by its early

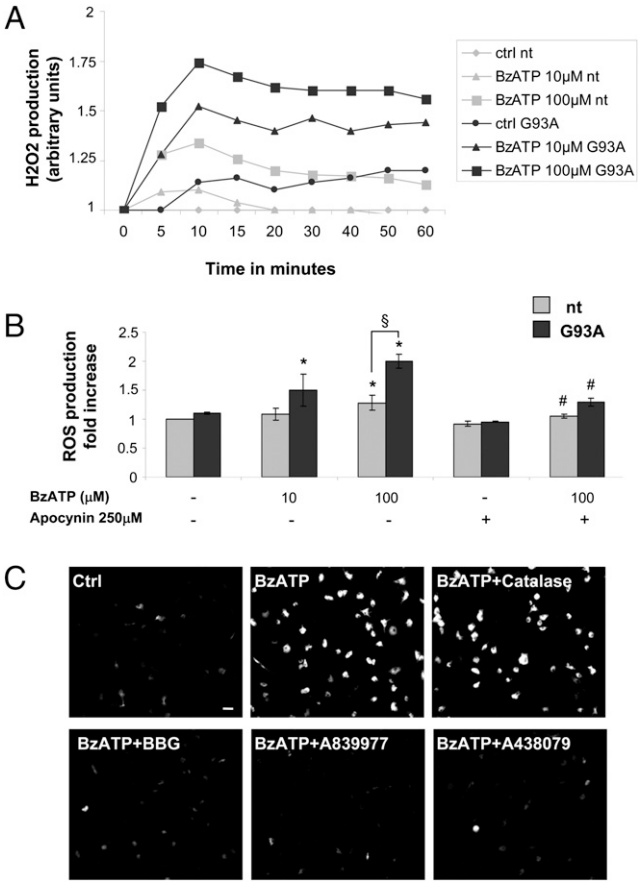

FIGURE 4. Modulation of the P2X$_7$ receptor alters ROS production in SOD1-G93A microglia. SOD1-G93A and nt microglia were plated onto a 96-well plate in serum-free medium, and H_2O_2 released from microglial cells stimulated with BzATP (10–100 μM) (**A**, **B**) in the presence of 250 μM apocynin (B) was determined by measuring Amplex Red fluorescence every 5 min (A) or after 10 min (B). Data represent mean ± SEM of $n = 3$ independent experiments. (**C**) Representative images of CellROX Deep Red Reagent fluorescence in SOD1-G93A microglia treated or not with 100 μM BzATP for 30 min, in the absence or presence of 1 μM BBG, A839977, or A438079. Fluorescence related to superoxide production was visualized after fixation using a confocal microscope. Scale bar, 50 μm. $^*p < 0.05$ versus nt untreated cells, $^§p < 0.05$ versus 100 μM BzATP–treated nt cells, $^\#p < 0.05$ versus 100 μM BzATP–treated SOD1-G93A cells, Student *t* test.

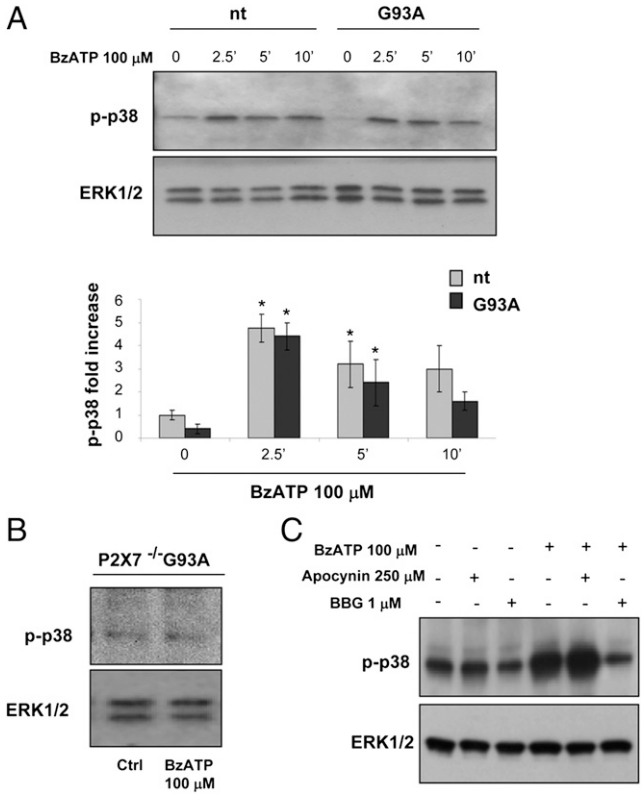

FIGURE 5. p38 is similarly activated by BzATP in SOD1-G93A and nt microglia. (**A**) SOD1-G93A and nt microglia were exposed to 100 μM BzATP for 2.5, 5, or 10 min, and equal amounts of total lysates were subjected to SDS-PAGE, Western blotting, and immunoreactions with anti–p-p38 and anti-ERK1/2 for protein normalization. Data represent mean ± SEM of $n = 3$ independent experiments. After 2.5 min of 100 μM BzATP stimulation, levels of p-p38 were analyzed by Western blot in P2X$_7^{-/-}$/SOD1-G93A (**B**) and in SOD1-G93A microglia pretreated with 1 μM BBG or 250 μM apocynin (**C**). $^*p < 0.05$ versus nt untreated cells, Student *t* test.

activation, we measured the phosphorylation of p38 in the presence of 250 μM apocynin. As shown in Fig. 5B, 100 μM BzATP is still effective in stimulating p38 activity, even upon pretreatment with the NOX2 inhibitor, indicating that this event is upstream or independent from NOX2 activity.

Differently from what we observed with p38, the phosphorylation of ERK1/2 induced by 100 μM BzATP is augmented in SOD1-G93A microglia with respect to nt cells. As shown in the time-course experiments in Fig. 6, ERK1/2 start to be significantly phosphorylated after 10 min of treatment, but the amount of p-ERK1/2 (normalized to total ERK1/2) is higher in SOD1-G93A cells than in nt cells (5- and 3-fold increase over control, respectively) (Fig. 6A); ERK1/2 phosphorylation peaks at 60 min, exhibiting a 6- and 4.5-fold increase in SOD1-G93A and nt cells, respectively, over control and then decreases nearly to control levels after 120 min (Fig. 6B). The addition of 1 μM BBG returns ERK1/2 phosphorylation to basal levels at 30 min of stimulation and inhibits the phosphorylation in SOD1-G93A microglia by ~70% at 60 min (Fig. 7A). In these cells, the addition of 1 μM A-839977 or A-438079 returns p-ERK1/2 to control levels after 60 min of BzATP stimulation (Fig. 7A). Moreover, in P2X$_7^{-/-}$/SOD1-G93A microglia, the addition of 100 μM BzATP for up to 60 min does not modify the levels of p-ERK1/2 (Fig. 7A). These data strongly indicate that the P2X$_7$ receptor mediates the phosphorylation of ERK1/2 induced by BzATP. Because ERK1/2 activation by BzATP seems to be a late event, peaking at 60 min, we analyzed whether it could rely on NOX2 activation (Fig. 7B). In cells pretreated with 250 μM apocynin, ERK1/2 phosphorylation is reduced by 30% at both 30 and 60 min of stimulation with BzATP. This result suggests that, at least in part, ERK1/2 phosphorylation by BzATP lies downstream of NOX2 activation. Conversely, we also tested whether inhibition of ERK1/2 phosphorylation could affect ROS production (Fig. 7C). As shown by fluorescence staining with CellROX Deep Red Reagent, ROS induction by 100 μM BzATP is clearly reduced by preincubation of SOD1-G93A microglia with the MEK pathway inhibitor PD98059, indicating that ERK1/2 activation is responsible, at least in part, for ROS production by BzATP. Overall, these data reveal a mutual dependency of NOX2 and ERK1/2 upon P2X$_7$ receptor stimulation in SOD1-G93A microglia (Fig. 8).

Discussion

The aim of this work was to decode the main molecular pathways modulated by the P2X$_7$ receptor that could account for neuro-

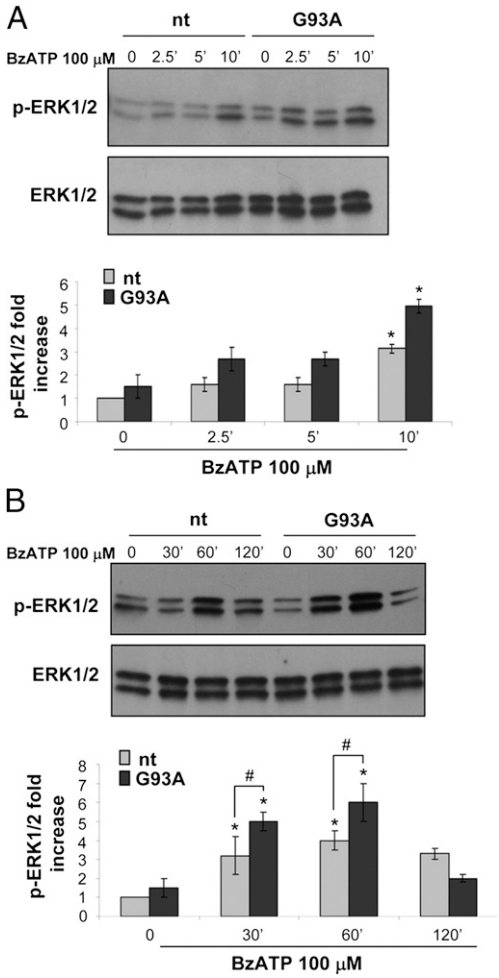

FIGURE 6. Phosphorylation of ERK1/2 by BzATP is significantly different in SOD1-G93A microglia compared with nt microglia. SOD1-G93A and nt microglia were exposed to 100 μM BzATP for 2.5, 5, or 10 min (**A**) and for 30, 60, or 120 min (**B**), and equal amounts of total lysates were subjected to SDS-PAGE, Western blotting, and immunoreactions with anti–p-ERK1/2 and anti–ERK1/2 for protein normalization. Data represent mean ± SEM of $n = 3$ independent experiments. $^{*}p < 0.05$ versus nt untreated cells, $^{\#}p < 0.05$ versus 100 μM BzATP–treated nt counterpart, Student t test.

inflammation during ALS pathogenesis and to identify early signaling targets and effectors that might be useful in intercepting the progression of the pathology. To this end, we made use of primary microglial cells derived from transgenic SOD1-G93A mice and SOD1-G93A mice lacking the $P2X_7$ receptor as models to investigate the effects of pharmacological induction or genetic ablation of the receptor activity. We found that $P2X_7$ receptor stimulation in SOD1-G93A microglia increases NOX2 activity, ROS production, and GTP-Rac1 and p-ERK1/2 levels. Based on our results, we propose a novel mechanism by which the $P2X_7$ receptor may lead to enhanced oxidative stress in ALS microglia. $P2X_7$ receptor stimulated by extracellular ATP directly activates ERK1/2 and NOX2, and both of these pathways converge in ROS generation; the induction of NOX2 relies on GTP-Rac1 and determines further ERK1/2 phosphorylation, with consequent ROS overproduction. This mechanism is consistent with what is already known about the $P2X_7$ receptor in ALS and with the pathway of NOX2 activation by ALS-related genes. Indeed, in a previous work we demonstrated that the extracellular ATP pool is better preserved and the $P2X_7$ receptor is upregulated in SOD1-G93A microglia, which translates into an increase in released proinflammatory factors and neurotoxicity induced by microglia upon $P2X_7$ receptor stimulation (21). In addition, several reports describe NOX2 as a source of damaging ROS in ALS (7, 9, 10, 12). Consistent with this, in the present study we found a basal upregulation of the Rac1-NOX2 pathway in the model of SOD1-G93A primary microglia, in line with previous results obtained in cell lines transiently infected with ALS-related genes (7, 12), and we also demonstrated that activation of the $P2X_7$ receptor further enhances this pathway, thus producing additional oxidative stress. Furthermore, by overexpression of a dominant-negative or constitutively active form of Rac1 in ALS microglia, we established that $p67^{phox}$ subunit translocation on membranes is totally dependent on Rac1 recruitment and not on alternative pathways; thus, Rac1 activation is a prerequisite for NOX2 activation by the $P2X_7$ receptor.

Because NOX2-derived ROS may activate MAPKs, which are known to be the core of the cell stress–response signaling network and, conversely, that oxidative stress also can occur through activation of MAPKs (28), we investigated the role of these relevant kinases, in particular p38 and ERK1/2, which are known to be activated by the $P2X_7$ receptor in microglial cells (29) and to be implicated in ALS pathology (30, 31). Although the role for ERK1/2 in ALS is controversial, being overphosphorylated or dephosphorylated in different cells and conditions (32–34), persistent activation of p38 signaling was suggested to mediate neuronal apoptosis in ALS. Indeed, increased levels of p-p38 MAPKs are present in the motor neurons and microglia of the ventral spinal cord of mutant SOD1 mice, and p38 inhibition largely protects motor neurons and prevents proximal axon degeneration (35). In this study, we found that, following $P2X_7$ receptor stimulation, the phosphorylation of ERK1/2 is augmented particularly in ALS microglia, and this effect is inhibited by the ROS inhibitor apocynin. We also demonstrated that inhibition of ERK1/2 phosphorylation decreases ROS production, suggesting a mutual dependency between ERK1/2 and NOX2 upon $P2X_7$ receptor stimulation. In these same experimental conditions, activation of p38 by BzATP is comparable in SOD1-G93A and healthy microglia. This may be explained by the fact that several kinases, in addition to MAPKs, such as protein kinase C, PAK, Akt and PI3K, may be involved in NOX2 activation (28). This complexity in the phosphorylation of $p47^{phox}$ and $p67^{phox}$ suggests that the intracellular signaling pathways responsible for this event may be cell type and stimulus specific. Taken together, all of these data led us to hypothesize that, in SOD1-G93A mice, ATP released in vivo in the surrounding extracellular space of damaged motor neurons and slowly hydrolyzed in the proximity of microglia overactivates the $P2X_7$ receptor, which is highly expressed in these cells, leading to oxidative stress via the Rac1-NOX2 and ERK1/2 pathways, as well as to the induction of proinflammatory factors. This effect adds to ROS production and activation of proinflammatory signals exerted by SOD1-G93A protein, causing further detrimental effects on the surrounding motor neurons.

Our findings contribute to improving the understanding of the biological processes that cause neuroinflammation in ALS and identify the $P2X_7$ receptor as a promising target to halt the vicious cycle between uncontrolled neuroinflammation and neuron degeneration, because its inactivation affects the earliest steps of the proinflammatory action exerted by ALS microglia. The important role of microglia in the progression of ALS has been widely recognized (36); indeed, a substantial slowing of disease progression was obtained by excision of mutant SOD1 in the myeloid lineage of SOD1-G93A mice (37). However, treatment with traditional nonsteroidal anti-inflammatory drugs, with minocycline and apocynin, or the knocking down of specific components of the

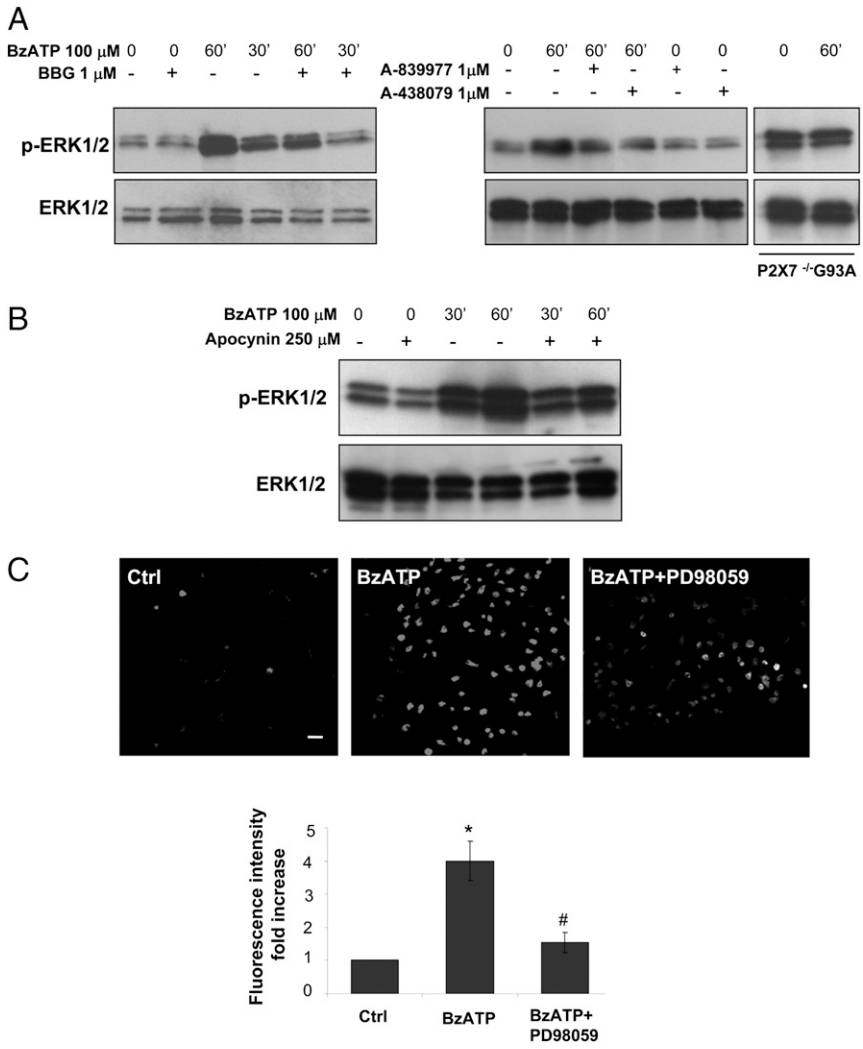

FIGURE 7. Mutual dependency between ERK1/2 and ROS by P2X$_7$ receptor activation in SOD1-G93A microglia. (**A** and **B**) SOD1-G93A and P2X$_7^{-/-}$/SOD1-G93A microglia were exposed to 100 μM BzATP for the indicated times, and Western blotting for anti–p-ERK and anti-ERK1/2 was performed. SOD1-G93A microglia were pretreated or not with 1 μM BBG, A-839977, or A-438079 (A) or with 250 μM apocynin (B). (**C**) CellROX Deep Red Reagent fluorescence related to superoxide production was visualized using a confocal microscope in SOD1-G93A microglia pretreated with 100 μM PD98059 and exposed to 100 μM BzATP for 60 min. CellROX Deep Red Reagent fluorescence intensities were measured using ImageJ software; data are representative of mean ± SEM of $n = 3$ independent experiments. Scale bar, 50 μm. $^*p < 0.05$ versus untreated cells, $^{\#}p < 0.05$ versus BzATP-treated cells, Student t test.

inflammatory pathway did not yield satisfactory results (38–40), suggesting that a successful inhibition of microglia-mediated toxicity might require the attenuation of a broad spectrum of different pathways. In this study, we show that inhibition of the P2X$_7$ receptor by genetic ablation or through the antagonists BBG, A-839977, and A-438079 suppress both early and late proinflammatory responses activated by BzATP in SOD1-G93A microglia (i.e., p67^{phox} translocation, p-ERK1/2 levels, and overall ROS production). Moreover, we showed that BBG significantly inhibits GTP-Rac1 activation and, to a lesser extent, the translocation of p67^{phox}, also in unstimulated conditions, suggesting that endogenous release of ATP might contribute to SOD1-G93A microglia basal activation (21) through stimulation of the P2X$_7$ receptor. Altogether, these results could be the rationale for a preclinical study using A-839977 or BBG in ALS mice, because they can cross the blood–brain barrier (41, 42). Moreover, it is known that BBG has no toxicity and exhibits therapeutic effects in other animal models of neurodegenerative diseases (42). However, one complicating factor in inhibiting the action of the P2X$_7$ receptor in vivo might result from the dichotomous role exerted by microglia in neurodegenerative diseases, such as ALS: initially, microglia have a neuroprotective action, clearing the source of the inflammatory stimuli (a condition known as M2 phenotype), whereas they transform into a toxic M1 phenotype that contributes to the acceleration of motor neuron degeneration (2, 43). Therefore, the challenge will be to inhibit the P2X$_7$ receptor only when microglia convert to the dangerous M1 phenotype and have a detrimental role, and to preserve the neuroprotective aspect. In summary, we confirmed the P2X$_7$ receptor as a promising target

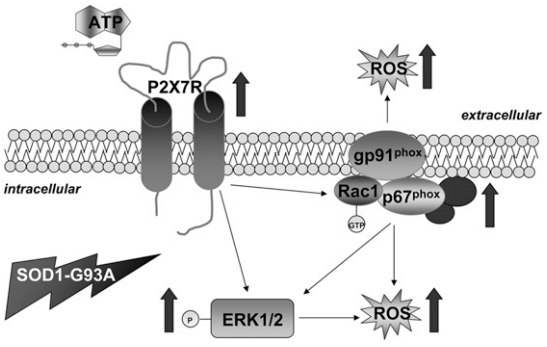

FIGURE 8. Schematic representation of P2X$_7$ receptor–NOX2–signaling pathway in SOD1-G93A microglia. In SOD1-G93A microglia, P2X$_7$ receptor stimulation by extracellular ATP increases GTP-bound Rac1 and, consequently, the translocation of p67^{phox} subunit to gp91^{phox} on cell membranes to form the active NOX2 complex. The active complex transports electrons across membranes to extracellular or endosomal oxygen, generating extracellular and intracellular ROS. Contextually, activation of the P2X$_7$ receptor leads to ERK1/2 phosphorylation, which determines a further generation of intracellular ROS. Moreover, the active NOX2 complex converges into ERK1/2 stimulation, eventually causing a boost in ROS.

for the development of therapeutic strategies to slow down the progression of ALS.

Disclosures

The authors have no financial conflicts of interest.

References

1. Cozzolino, M., M. G. Pesaresi, V. Gerbino, J. Grosskreutz, and M. T. Carrì. 2012. Amyotrophic lateral sclerosis: new insights into underlying molecular mechanisms and opportunities for therapeutic intervention. *Antioxid. Redox Signal.* 17: 1277–1330.
2. Henkel, J. S., D. R. Beers, W. Zhao, and S. H. Appel. 2009. Microglia in ALS: the good, the bad, and the resting. *J. Neuroimmune Pharmacol.* 4: 389–398.
3. Ilieva, H., M. Polymenidou, and D. W. Cleveland. 2009. Non-cell autonomous toxicity in neurodegenerative disorders: ALS and beyond. *J. Cell Biol.* 187: 761–772.
4. Bedard, K., and K. H. Krause. 2007. The NOX family of ROS-generating NADPH oxidases: physiology and pathophysiology. *Physiol. Rev.* 87: 245–313.
5. Block, M. L. 2008. NADPH oxidase as a therapeutic target in Alzheimer's disease. *BMC Neurosci.* 9(Suppl. 2): S8.
6. Hordijk, P. L. 2006. Regulation of NADPH oxidases: the role of Rac proteins. *Circ. Res.* 98: 453–462.
7. Harraz, M. M., J. J. Marden, W. Zhou, Y. Zhang, A. Williams, V. S. Sharov, K. Nelson, M. Luo, H. Paulson, C. Schöneich, and J. F. Engelhardt. 2008. SOD1 mutations disrupt redox-sensitive Rac regulation of NADPH oxidase in a familial ALS model. *J. Clin. Invest.* 118: 659–670.
8. Boillée, S., and D. W. Cleveland. 2008. Revisiting oxidative damage in ALS: microglia, Nox, and mutant SOD1. *J. Clin. Invest.* 118: 474–478.
9. Wu, D. C., D. B. Ré, M. Nagai, H. Ischiropoulos, and S. Przedborski. 2006. The inflammatory NADPH oxidase enzyme modulates motor neuron degeneration in amyotrophic lateral sclerosis mice. *Proc. Natl. Acad. Sci. USA* 103: 12132–12137.
10. Marden, J. J., M. M. Harraz, A. J. Williams, K. Nelson, M. Luo, H. Paulson, and J. F. Engelhardt. 2007. Redox modifier genes in amyotrophic lateral sclerosis in mice. *J. Clin. Invest.* 117: 2913–2919.
11. Valdmanis, P. N., E. Kabashi, P. A. Dion, and G. A. Rouleau. 2008. ALS predisposition modifiers: knock NOX, who's there? SOD1 mice still are. *Eur. J. Hum. Genet.* 16: 140–142.
12. Li, Q., N. Y. Spencer, N. J. Pantazis, and J. F. Engelhardt. 2011. Alsin and SOD1 (G93A) proteins regulate endosomal reactive oxygen species production by glial cells and proinflammatory pathways responsible for neurotoxicity. *J. Biol. Chem.* 286: 40151–40162.
13. Di Virgilio, F., S. Ceruti, P. Bramanti, and M. P. Abbracchio. 2009. Purinergic signalling in inflammation of the central nervous system. *Trends Neurosci.* 32: 79–87.
14. Skaper, S. D., P. Debetto, and P. Giusti. 2010. The P2X7 purinergic receptor: from physiology to neurological disorders. *FASEB J.* 24: 337–345.
15. Weisman, G. A., J. M. Camden, T. S. Peterson, D. Ajit, L. T. Woods, and L. Erb. 2012. P2 receptors for extracellular nucleotides in the central nervous system: role of P2X7 and $P2Y_2$ receptor interactions in neuroinflammation. *Mol. Neurobiol.* 46: 96–113.
16. Volonté, C., S. Apolloni, S. D. Skaper, and G. Burnstock. 2012. P2X7 receptors: channels, pores and more. *CNS Neurol. Disord. Drug Targets* 11: 705–721.
17. Volonté, C., S. Apolloni, M. T. Carrì, and N. D'Ambrosi. 2011. ALS: focus on purinergic signalling. *Pharmacol. Ther.* 132: 111–122.
18. Amadio, S., S. Apolloni, N. D'Ambrosi, and C. Volonté. 2011. Purinergic signalling at the plasma membrane: a multipurpose and multidirectional mode to deal with amyotrophic lateral sclerosis and multiple sclerosis. *J. Neurochem.* 116: 796–805.
19. Yiangou, Y., P. Facer, P. Durrenberger, I. P. Chessell, A. Naylor, C. Bountra, R. R. Banati, and P. Anand. 2006. COX-2, CB2 and P2X7-immunoreactivities are increased in activated microglial cells/macrophages of multiple sclerosis and amyotrophic lateral sclerosis spinal cord. *BMC Neurol.* 6: 12.
20. Casanovas, A., S. Hernández, O. Tarabal, J. Rosselló, and J. E. Esquerda. 2008. Strong P2X4 purinergic receptor-like immunoreactivity is selectively associated with degenerating neurons in transgenic rodent models of amyotrophic lateral sclerosis. *J. Comp. Neurol.* 506: 75–92.
21. D'Ambrosi, N., P. Finocchi, S. Apolloni, M. Cozzolino, A. Ferri, V. Padovano, G. Pietrini, M. T. Carrì, and C. Volonté. 2009. The proinflammatory action of microglial P2 receptors is enhanced in SOD1 models for amyotrophic lateral sclerosis. *J. Immunol.* 183: 4648–4656.
22. Gandelman, M., H. Peluffo, J. S. Beckman, P. Cassina, and L. Barbeito. 2010. Extracellular ATP and the P2X7 receptor in astrocyte-mediated motor neuron death: implications for amyotrophic lateral sclerosis. *J. Neuroinflammation* 7: 33.
23. Saura, J., J. M. Tusell, and J. Serratosa. 2003. High-yield isolation of murine microglia by mild trypsinization. *Glia* 44: 183–189.
24. Cozzolino, M., V. Stagni, L. Spinardi, N. Campioni, C. Fiorentini, E. Salvati, S. Alemà, and A. M. Salvatore. 2003. p120 Catenin is required for growth factor-dependent cell motility and scattering in epithelial cells. *Mol. Biol. Cell* 14: 1964–1977.
25. Kalyanaraman, B., V. Darley-Usmar, K. J. Davies, P. A. Dennery, H. J. Forman, M. B. Grisham, G. E. Mann, K. Moore, L. J. Roberts, II, and H. Ischiropoulos. 2012. Measuring reactive oxygen and nitrogen species with fluorescent probes: challenges and limitations. *Free Radic. Biol. Med.* 52: 1–6.
26. Leto, T. L., S. Morand, D. Hurt, and T. Ueyama. 2009. Targeting and regulation of reactive oxygen species generation by Nox family NADPH oxidases. *Antioxid. Redox Signal.* 11: 2607–2619.
27. Allen, W. E., G. E. Jones, J. W. Pollard, and A. J. Ridley. 1997. Rho, Rac and Cdc42 regulate actin organization and cell adhesion in macrophages. *J. Cell Sci.* 110: 707–720.
28. Wilkinson, B. L., and G. E. Landreth. 2006. The microglial NADPH oxidase complex as a source of oxidative stress in Alzheimer's disease. *J. Neuroinflammation* 3: 30.
29. Friedle, S. A., V. M. Brautigam, M. Nikodemova, M. L. Wright, and J. J. Watters. 2011. The P2X7-Egr pathway regulates nucleotide-dependent inflammatory gene expression in microglia. *Glia* 59: 1–13.
30. Kim, E. K., and E. J. Choi. 2010. Pathological roles of MAPK signaling pathways in human diseases. *Biochim. Biophys. Acta* 1802: 396–405.
31. Chung, Y. H., K. M. Joo, H. C. Lim, M. H. Cho, D. Kim, W. B. Lee, and C. I. Cha. 2005. Immunohistochemical study on the distribution of phosphorylated extracellular signal-regulated kinase (ERK) in the central nervous system of SOD1G93A transgenic mice. *Brain Res.* 1050: 203–209.
32. Ayala, V., A. B. Granado-Serrano, D. Cacabelos, A. Naudí, E. V. Ilieva, J. Boada, V. Caraballo-Miralles, J. Lladó, I. Ferrer, R. Pamplona, and M. Portero-Otin. 2011. Cell stress induces TDP-43 pathological changes associated with ERK1/2 dysfunction: implications in ALS. *Acta Neuropathol.* 122: 259–270.
33. Perlson, E., G. B. Jeong, J. L. Ross, R. Dixit, K. E. Wallace, R. G. Kalb, and E. L. Holzbaur. 2009. A switch in retrograde signaling from survival to stress in rapid-onset neurodegeneration. *J. Neurosci.* 29: 9903–9917.
34. Yang, E. J., J. H. Jiang, S. M. Lee, S. C. Yang, H. S. Hwang, M. S. Lee, and S. M. Choi. 2010. Bee venom attenuates neuroinflammatory events and extends survival in amyotrophic lateral sclerosis models. *J. Neuroinflammation* 7: 69.
35. Dewil, M., V. F. dela Cruz, L. Van Den Bosch, and W. Robberecht. 2007. Inhibition of p38 mitogen activated protein kinase activation and mutant SOD1 (G93A)-induced motor neuron death. *Neurobiol. Dis.* 26: 332–341.
36. Philips, T., and W. Robberecht. 2011. Neuroinflammation in amyotrophic lateral sclerosis: role of glial activation in motor neuron disease. *Lancet Neurol.* 10: 253–263.
37. Boillée, S., K. Yamanaka, C. S. Lobsiger, N. G. Copeland, N. A. Jenkins, G. Kassiotis, G. Kollias, and D. W. Cleveland. 2006. Onset and progression in inherited ALS determined by motor neurons and microglia. *Science* 312: 1389–1392.
38. Turner, B. J., and K. Talbot. 2008. Transgenics, toxicity and therapeutics in rodent models of mutant SOD1-mediated familial ALS. *Prog. Neurobiol.* 85: 94–134.
39. Riboldi, G., M. Nizzardo, C. Simone, M. Falcone, N. Bresolin, G. P. Comi, and S. Corti. 2011. ALS genetic modifiers that increase survival of SOD1 mice and are suitable for therapeutic development. *Prog. Neurobiol.* 95: 133–148.
40. Phani, S., D. B. Re, and S. Przedborski. 2012. The Role of the Innate Immune System in ALS. *Front. Pharmacol.* 3: 150.
41. Honore, P., D. Donnelly-Roberts, M. Namovic, C. Zhong, C. Wade, P. Chandran, C. Zhu, W. Carroll, A. Perez-Medrano, Y. Iwakura, and M. F. Jarvis. 2009. The antihyperalgesic activity of a selective P2X7 receptor antagonist, A-839977, is lost in IL-1alphabeta knockout mice. *Behav. Brain Res.* 204: 77–81.
42. Takenouchi, T., K. Sekiyama, A. Sekigawa, M. Fujita, M. Waragai, S. Sugama, Y. Iwamaru, H. Kitani, and M. Hashimoto. 2010. P2X7 receptor signaling pathway as a therapeutic target for neurodegenerative diseases. *Arch. Immunol. Ther. Exp. (Warsz.)* 58: 91–96.
43. Liao, B., W. Zhao, D. R. Beers, J. S. Henkel, and S. H. Appel. 2012. Transformation from a neuroprotective to a neurotoxic microglial phenotype in a mouse model of ALS. *Exp. Neurol.* 237: 147–152.